Effect and measurement of residual water in CaCl2 intended for use as electrolyte in molten salt electrochemical processing

Faulkner, Emma
Monreal, Marisa Jennifer
Jackson, Jay Matthew
Simpson, Michael F.

To be published in: Journal of Radioanalytical and Nuclear Chemistry

DOI to publisher's version: 10.1007/s10967-020-07413-0

Title Page

Names of authors:	Emma Faulkner[1], Marisa Monreal[2], Matt Jackson[2], and *Michael F. Simpson[1]
Title:	Effect and Measurement of Residual Water in $CaCl_2$ Intended for Use as Electrolyte in Molten Salt Electrochemical Processing
Affiliations of authors:	[1]University of Utah, Department of Materials Science & Engineering, Salt Lake City, UT, USA
	[2]Los Alamos National Laboratory, Los Alamos, NM, USA
Corresponding author:	Michael Simpson (michael.simpson@utah.edu)

Effect and Measurement of Residual Water in $CaCl_2$ Intended for Use as Electrolyte in Molten Salt Electrochemical Processing

Emma Faulkner[1], Marisa Monreal[2], Matt Jackson[2], and Michael F. Simpson[1]

[1]University of Utah, Department of Materials Science & Engineering, Salt Lake City, UT, USA

[2]Los Alamos National Laboratory, Los Alamos, NM, USA

Abstract

$CaCl_2$ has applications for electrochemical processing of nuclear materials. Thermal dehydration leads to formation of oxide ions, which are shown to react and cause precipitation of dissolved $CeCl_3$ that was selected as a surrogate for actinide chlorides. Thus, measurement of residual water in $CaCl_2$ is an essential capability. Thermogravimetric analysis (TGA) was shown to underestimate starting water concentration. Subsequent analysis of solid samples via acid-base titration and cyclic voltammetry (CV) of the molten salt yielded consistent values within 5% for residual water. Hydroxides were shown to be unstable, thus oxygen is retained as oxide ions. Thus, total water in a sample of $CaCl_2$ can be quantified by combining TGA with with either CV of molten salt or titration of salt samples. The importance of quantifying residual water in the salt was demonstrated by showing that cerium chloride (surrogate for actinide chlorides) will react with oxide ions in $CaCl_2$ to form insoluble oxides and oxychlorides.

Keywords: molten salt, electrorefining, actinide purification, high temperature electrochemistry

Introduction

Molten $CaCl_2$ has numerous viable applications pertaining to advanced systems for energy conversion and storage. This includes thermal energy storage [1], grid-scale molten metal batteries [2], and processing/purification of nuclear materials [3, 4].

In the last of these examples, molten $CaCl_2$ can be used as an electrolyte for reducing U and/or Pu oxides, in addition to electrorefining U and/or Pu metals [5]. Electrorefining reactions using plutonium as the metal are given below as examples.

$$Pu_{(l)} = Pu^{3+}_{(salt)} + 3e^- \ (anode) \quad (1)$$

$$Pu^{3+}_{(salt)} + 3e^- = Pu_{(l)} \ (cathode) \quad (2)$$

Such application for the electrolytic reduction of actinide oxides has been reported by researchers from Japan [3, 6]. Use of molten $CaCl_2$ for electrorefining U metal was first reported by Niedrach and Glamm from Knolls Atomic Power Laboratory in the 1950s [7]. A molten salt electrolyte mixture including $CaCl_2$ was initially considered for electrorefining irradiated Experimental Breeder Reactor-II fuel under the Integral Fast Reactor Program before the decision was eventually made to use eutectic LiCl-KCl [8].

Working with $CaCl_2$ for these applications is challenging because of the necessity to keep the salt dry. $CaCl_2$ is extremely hygroscopic and will take on up to six waters of hydration in contact with humid air [1]. Much of this water can be removed from small samples of salt powder by thermal dehydration with a very slow temperature ramp rate to 200°C [1]. But slow mass transfer of water from solid salt makes it impractical to completely dehydrate the salt before the melting transition at 772°C. Incomplete removal of the water can lead to a hydrolysis reaction, forming hydroxides or oxides in the molten salt [9, 10]. The following reactions are likely between water and molten $CaCl_2$.

$$CaCl_2 + 2H_2O \rightarrow Ca(OH)_2 + 2HCl \quad (3)$$

$$CaCl_2 + H_2O \rightarrow CaO + 2HCl \quad (4)$$

If an as-received batch of $CaCl_2$ contains some absorbed water, as would likely be the case due to the hygroscopic nature of the salt, quantification and removal of that water would be problematic. While a chemical supplier may claim a batch of $CaCl_2$ to be anhydrous with a specification such as 0.1% or less water, its actual water contamination may be much higher than

reported due to inadequate means of analysis. In order to overcome slow mass transfer of water due to solid state diffusion, the salt must be melted by heating above 772ºC so that it is molten. But at that temperature, it is hypothesized that reactions represented by Equations (3) and (4) can occur. Thus, simple thermal dehydration will increase the sum concentration of hydroxide and oxide in the salt. This prevents quantification of the initial water content by gravimetric means. In other words, mass loss cannot be directly equated to mass of water lost.

It is likely that only CaO is present in the salt because the decomposition of $Ca(OH)_2$ occurs around 400°C, as follows [11, 12]:

$$Ca(OH)_2 \rightarrow CaO + H_2O \quad (5)$$

If this reaction also occurs in $CaCl_2$-$Ca(OH)_2$ molten salt mixtures, then the possible presence of hydroxide in the salt as a contaminant can be ignored. The only oxygen-based contaminant would be CaO. Note that it has been reported by Kondo et. al. that $Ca(OH)_2$ is stable in molten $CaCl_2$ when in contact with water vapor [13]. But those conditions do not apply in this study where the salt would be either dried in vacuum or in contact with dry argon gas. The work reported by Kondo et. al. is also key for identifying that reactions (3) and (4) occur. If the salt is intended for use in the electrolytic oxide reduction process, CaO is intentionally added at a relatively high concentration (1 wt%), meaning that the incidental contamination of $CaCl_2$ with CaO from dehydration is likely inconsequential. However, if the $CaCl_2$ is intended to be used for electrorefining, such CaO contamination cannot be ignored and must be minimized to avoid reaction with actinide chlorides to form insoluble oxides or oxychlorides [6]. In the uranium/plutonium electrorefining process, CaO is expected to react with UCl_3 and $PuCl_3$ to form insoluble oxides and/or oxychlorides. One example of a possible reaction between plutonium chloride in the ER salt with CaO is given in equation (4), which has a ΔG^o_{rxn} of -214.9 kJ/mole at 850ºC assuming super cooled liquid states for $PuCl_3$, CaO, and $CaCl_2$ [14].

$$PuCl_{3(salt)} + CaO_{(salt)} = PuOCl_{(solid)} + CaCl_{2(salt)} \quad (6)$$

The goals of this study are to develop a method of water/oxide/hydroxide analysis in $CaCl_2$ and determine the impact of oxides/hydroxides on dissolved actinide chlorides. Cerium was studied as a surrogate for actinides. This should establish the need for using enhanced salt purification processes such as hydrochlorination prior to using the salt for processing nuclear materials. Three methods are reported—cyclic voltammetry (CV) of the molten salt mixture, thermogravimetric analysis (TGA) of salt samples, and titration of salt samples. A method for determining the total concentration of water in a sample of $CaCl_2$ is reported that combines TGA of the as-received salt combined with titration or CV of the melted salt. The importance of the application of this salt to processing/purifying actinides is well established. But there has not been a systematic way to measure residual water in the salt prior to melting and use. The results of this study are, thus, needed to enable more consistent reporting of electrochemical actinide processing in molten $CaCl_2$.

Experimental

Chemicals

Anhydrous $CaCl_2$ (APL Engineered Materials, 99.9%) was used as received. In electrochemical tests, the salt was contained in 4.4 cm-diameter yttria stabilized MgO crucibles (Tateho Ozark, 99.2%). CaO (Fisher Scientific, >99.95%), $Ca(OH)_2$ (Fisher Scientific, >96%) and anhydrous $CeCl_3$ (Alfa Aesar, >99.9%) were used as received. Trace metal grade HCl and HNO_3 (Fisher Scientific) were used for titration and ICP-MS sample preparation.

Equipment

Salts were handled and electrochemical tests were carried out inside an Innovative Technologies PureLab glovebox with argon atmosphere (<1 ppm H_2O, <1 ppm O_2). For each electrochemical analysis experiment 65-75 g of salt was added to the inner MgO crucible, which has a 4.4 cm outer diameter. The inner crucible was nested into an outer MgO crucible with a 7.6 cm outer diameter. For these experiments, the salt was heated to 850 ±5°C at a rate of 1.5 °C/min

with a Thermolyne 1300 muffle furnace modified by cutting a 10-cm-diam hole in the top to allow for electrode insertions from above, as shown in Figure 1. A heat shield was formed consisting of two plates screwed together with six parallel holes, through which were inserted three alumina tubes. The tubes served as guides for metal electrodes. A three-electrode setup was used for cyclic voltammetry with 2-mm-diam tungsten (Alfa Aesar, 99.95%) rods acting as the working-, counter-, and quasi-reference electrodes.

Solution resistance between the working electrode (WE) and reference electrode (RE) was measured via an electrical impedance spectroscopy (EIS) method using a Gamry Reference 600+ potentiostat, and all CV was performed with an Autolab PGSTAT302N potentiostat. A vertical translator featuring a Velmex X-slide was used to precisely control the depth of the working electrode for an accurate estimate of surface area, as described elsewhere [15]. The WE surface area for the measurements varied from 0.5-1 cm^2. In the results section, WE area is not given for every experiment. But the area was divided into the current data from the CV runs to yield current density, which is what is actually plotted. Furnace temperature was verified using an ungrounded k-type thermocouple from Omega (Catalog Number KQXL-116U-12) that was occasionally inserted into the salt and then removed. The thermocouple was not immersed in the salt during any of the electrochemical measurements.

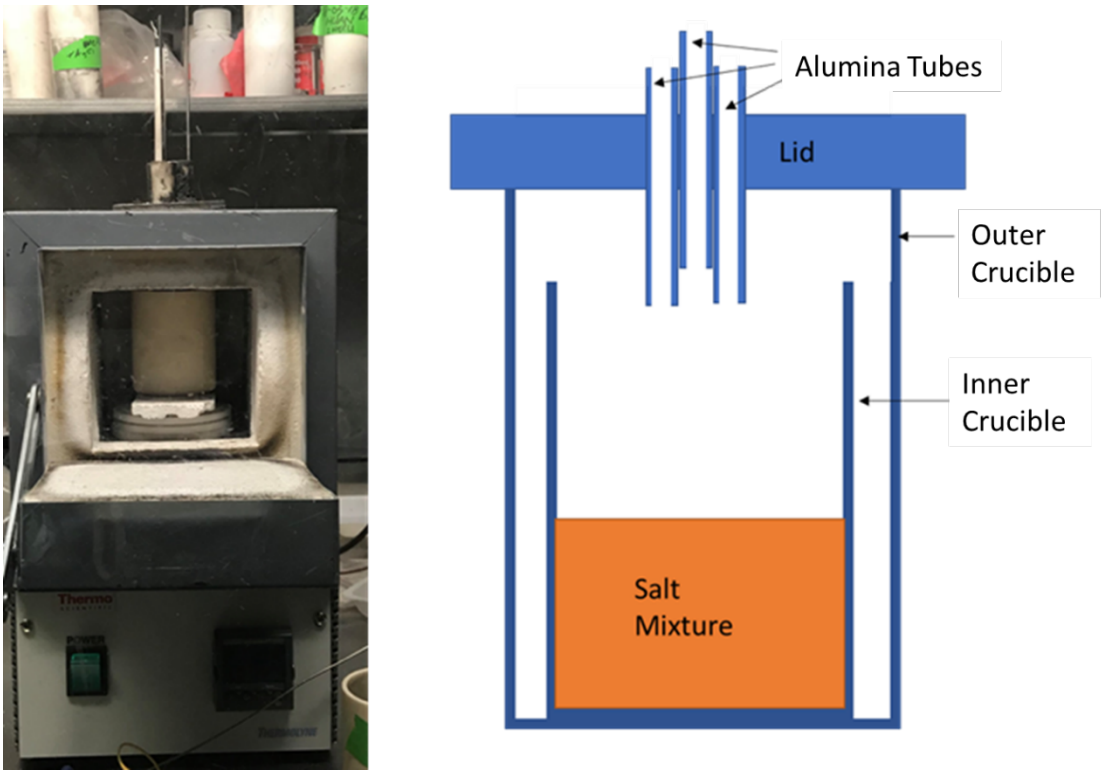

Fig. 1 Molten salt electrochemistry system shown in a photo (left) and diagram (right). The inner crucible was made of yttria stabilized magnesia. For scaling purposes, heated chamber shown in photo has dimensions of 8.5 cm high by 12.7 cm across. Inner crucible has a 4.4 cm outer diameter.

An SDT 650 TGA/DSC from TA Instruments was used for TGA of salt samples. X-ray diffraction was performed using a Philips PANalytical X-pert. Titrations were performed by dissolving salt samples in nanopure, deionized water and running a TitroLine 7000 with a BlueLine combination electrode (SI Analytics) in pH stat mode. The pH stat method used a setpoint of 2 and a titrant of 0.1 M HCl.

Methods

Cyclic voltammetry was performed with scan rates ranging from 100 to 600 mV/s, increasing in 50 mV/s increments. Potentials scanned ranged from -1.0 to 1.0 V. The solution resistance was measured in the range of 0.16–0.21 ohm, which appeared to depend on the

composition of the salt. This value was used in the Nova software (Version 2.1) to provide compensation for resistance.

Salt samples were analyzed with TGA to measure the amount of thermally desorbable water. The SDT-650 TGA was located outside of the glovebox in normal ambient atmospheric conditions. To minimize uptake of water before starting the TGA, salt samples were loaded into scintillation vials before being removed from the glovebox. After taring the sample cup, 10–20 mg of salt was placed in the cup, and the test began promptly. Samples for TGA were held in platinum cups (TA Instruments, part number 960149.901). All tests were performed with a carrier gas of ultra high purity argon (Airgas, catalog no. AR UHP300DS). TGA tests covered a temperature range of 50 to 850°C, at a heating rate of 20°C/min.

Titration was used to measure the amount of hydroxide formed when a salt sample was dissolved in water. As per the reaction shown in Equation (4), every oxide ion generated two hydroxide ions. Thus, the method yields incomplete information, as it cannot naturally distinguish between OH^- and O^{2-} in the salt.

$$O^{2-} + H_2O = 2OH^- \quad (7)$$

The pH-stat titration method was performed using a Titroline 7000 autotitrator with pH set point of 2 and a titrant of 0.1 M HCl. Masses of salt analyzed ranged from 0.5 to 0.8 g. Salt was collected using a room-temperature all-thread rod dipped in the molten salt. In order to avoid absorption of water in the salt samples, they were handled in the argon-atmosphere glove box until taken out and immediately titrated. If some water did absorb in the sample and reacted with CaO to form $Ca(OH)_2$, it would yield the same titration result as if no water had been absorbed.

For composition analysis of salts containing cerium chloride by inductively coupled plasma mass spectrometry (ICP-MS), salt samples were collected from molten salt by dipping and quickly withdrawing a room-temperature all-thread rod. Solidified salt samples were broken off of the all-thread rod and stored in sealed bottles in the glovebox. The collected salts were dissolved in a solution of 5% HCl and 5% HNO_3 and diluted to an estimated cerium concentration of 100–500 ppb. ICP-MS (Agilent ICP-MS 7900) was used to measure the actual concentration of cerium.

Standards were prepared using 100 µg/mL cerium from Inorganic Ventures. The concentrations used were 0.1, 1, 10, 100, 1000, and a blank of only 2% HNO_3.

Phases present in the salt were identified using X-ray diffraction (XRD, Philips PANalytical X-Pert). The MgO crucible containing the salt was cracked open with a hammer and then struck again to separate the bottom layer of the salt. The separated chunks of salt were ground with a mortar and pestle to a fine size suitable for XRD. The powder was placed in a scintillation vial and removed from the glovebox and then removed and placed on the slide immediately before testing. No other measures were taken to prevent contact with air. The 2θ angle range was 20–80°, at a rate of 1°/min.

Results and Discussion

Evaluation of Water Contamination in $CaCl_2$

If it is known that only water is coming off a sample due to increasing its temperature in a TGA, then the weight loss recorded can be directly attributed to water loss. Water may simply be desorbed, or it can be formed via the hydroxide decomposition reaction shown in Equation (3).

It has been reported that pure $Ca(OH)_2$ undergoes decomposition at about 400°C [11, 12]. Roughly 20% mass loss occurs as $Ca(OH)_2$ decomposes into CaO and H_2O, ending at a temperature of 600°C as reported by Yan and Zhao [11]. A complete decomposition would require a 24% weight loss. To determine if this decomposition reaction also occurs in a $CaCl_2$-$Ca(OH)_2$ molten salt solution, a powder mixture of 10% by weight $Ca(OH)_2$ in $CaCl_2$ was prepared and tested using thermogravimetric analysis (Figure 2). This is a much higher concentration of $Ca(OH)_2$ than would be expected as an impurity in the $CaCl_2$, but the concentration needed to be maximized in order to accurately measure the mass loss due to hydroxide decomposition. Anhydrous $CaCl_2$ before and after adding 10 wt% $Ca(OH)_2$, was heated in the TGA to 800°C. The results are overlaid in Figure 2. The anhydrous $CaCl_2$ lost 0.75% mass over the entire temperature range. The $CaCl_2$-$Ca(OH)_2$ lost 0.5% mass by 100°C, experienced very little mass loss between 100 and 350°C, and then lost an additional 2.04% mass between 350 and 525°C. The 2.04% mass loss in the $CaCl_2$-$Ca(OH)_2$ is consistent with the 20% mass lost from heating pure $Ca(OH)_2$

223 reported by Yan and Zhao. Thus, it appears that $Ca(OH)_2$ thermal decomposition occurs much the
224 same whether pure or mixed with $CaCl_2$. Note that the measurement error for TGA is +/- 0.5% as
225 reported by the manufacturer.

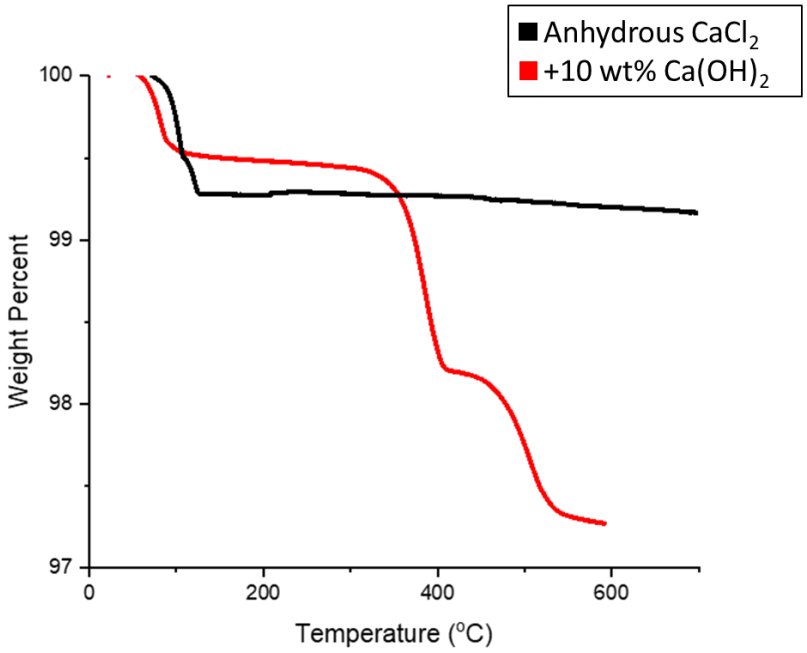

226

227 **Fig. 2** Mass loss comparison of anhydrous $CaCl_2$ and anhydrous $CaCl_2$ with 10 wt% $Ca(OH)_2$

228 In order to further test the hypothesis that hydroxide is unstable in molten $CaCl_2$, a series
229 of CV scans were performed in $CaCl_2$ with known additions of CaO and $Ca(OH)_2$. An overlay of
230 the CV scans is shown in Figure 3. CaO additions were made to molten salt by pouring the CaO
231 through the furnace lid, while the much finer $Ca(OH)_2$ was added to cooled salt, as the powder was
232 harder to control. Prior to running CV on the salt containing $Ca(OH)_2$, the salt was reheated to
233 850°C and allowed to sit for about 2 hr. The oxidation peak at 0.4 V and reduction peak at 0 V
234 both grew with each addition of CaO. $Ca(OH)_2$ was added to the salt with 1.0 wt% CaO after the
235 salt had been cooled. Interestingly, the addition of $Ca(OH)_2$ caused the 0.4 V oxidation peak to
236 increase just as caused by CaO addition. This behavior is consistent with $Ca(OH)_2$ spontaneously
237 decomposing to CaO. Addition of $Ca(OH)_2$ causes the same change in the CV oxidation peak as
238 does CaO. Based on the percentage of conversion of $Ca(OH)_2$ to CaO reported by Yan and Zhao,
239 the $Ca(OH)_2$ decomposition should have increased the CaO concentration by 38% to 1.38 wt%.
240 Meanwhile, the oxidation peak increased in magnitude by 24%. Thus, both the TGA result (Figure
241 2) and CV result (Figure 3) indicate that hydroxide spontaneously decomposes to oxide in molten

calcium chloride. Based on Figure 2, that decomposition initiates at a temperature below the melting point of $CaCl_2$ (m.p. = 772ºC). These observations are consistent with those reported by Kondo et. al. regarding $Ca(OH)_2$ stability but do lower the applicable temperature range for decomposition in a dry atmosphere by about 50 K [13].

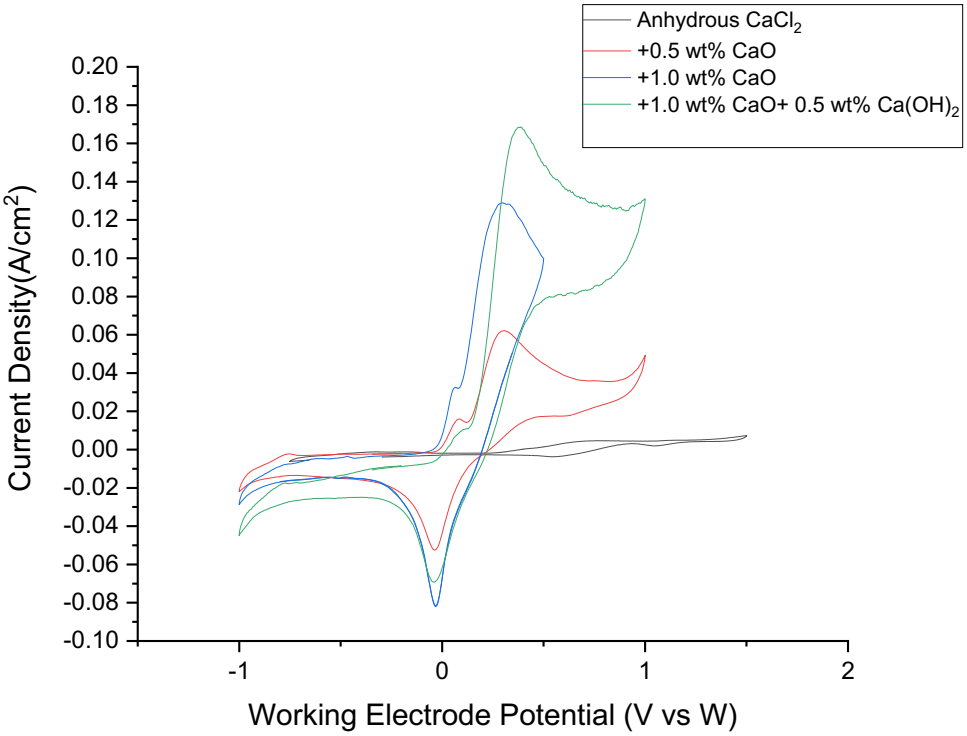

Fig. 3 CV in molten $CaCl_2$ with additions of CaO and $Ca(OH)_2$. Scans were performed at a scan rate of 300 mV/s, at a temperature of 850°C. Tungsten was used for all three electrodes, and the WE had a diameter of 2mm.

Measurement of Residual Water Concentration in Molten $CaCl_2$

The presumed hydrolysis of chloride salt before complete water desorption complicates the job of measuring the residual water content in a batch of salt. The chloride salt can be heated in a TGA to yield the wt% of desorbable water. But then some hydroxide decomposes to oxide. Weight loss due to water desorption and hydroxide decomposition cannot be clearly distinguished with TGA, unless it is assumed that a specific temperature exists and is known that divides water

desorption from hydroxide composition. Based on Figure 2, this occurs before 370°C. We propose a simple formula for quantifying the total molar water content (C_{tot} in units of moles H_2O/g salt) in a sample of $CaCl_2$, as follows in Equation (5). C_{des} is the concentration of desorbable water (moles H_2O/g salt), and C_{oxide} is the concentration of water that reacts to form oxide (moles H_2O/g salt).

$$C_{tot} = C_{des} + C_{oxide} \quad (8)$$

Given the previously presented evidence that $Ca(OH)_2$ is unstable in molten $CaCl_2$ and reverts to CaO, we endeavored to develop methods of measuring the CaO concentration that is equivalent to C_{oxide}, since there is a 1:1 molar ratio between H_2O and CaO in Equation (2). To make this measurement, two methods were investigated—acid titration and CV. The basis of the acid titration is that each mole of CaO should generate 2 moles of OH^- upon dissolution in water. As previously mentioned, the titration method cannot inherently distinguish between CaO and $Ca(OH)_2$. But now that it has been established that $Ca(OH)_2$ is not stable in the molten salt, titrations of samples taken of the molten salt should titrate only in response to CaO. The autotitrator was run in pH-stat mode at a pH set point of 2. After each salt sample was added to the titration cell, the auto-titrator added known volumes of HCl solution until the pH returned to the set point value. This method requires the salt to be melted and re-solidified before being analyzed. This allows for the residual water in the salt to react to form O^{2-}. If a sample of melted $CaCl_2$ is simply titrated, only O^{2-} originally in the salt will affect the titration, whereas titrating an as-received sample would include O^{2-} that has been adsorbed.

A series of experiments was performed in which known amounts of CaO were added to the anhydrous $CaCl_2$, melted, sampled, and titrated. Figure 4 plots the measured concentration of CaO (via titration) versus wt% CaO added. It also plots the calculated CaO concentration for each measured data point for comparison. The "calculated" line is just a unit conversion from the given wt% CaO to moles of CaO/g $CaCl_2$. It can be seen that the measured concentrations are linear with the amount of CaO added and that there is almost a constant off-set between the two lines. The y-intercept of the linear fit of the measured data is 3 x 10^{-5} mol CaO/g salt. This indicates a molar concentration of 3 x 10^{-5} mol CaO/g $CaCl_2$ present in the salt after melting. Assuming all of the

CaO came from H_2O reacting with $CaCl_2$, C_{oxide} can be inferred to be equal to 3 x 10^{-5} mol H_2O/g $CaCl_2$.

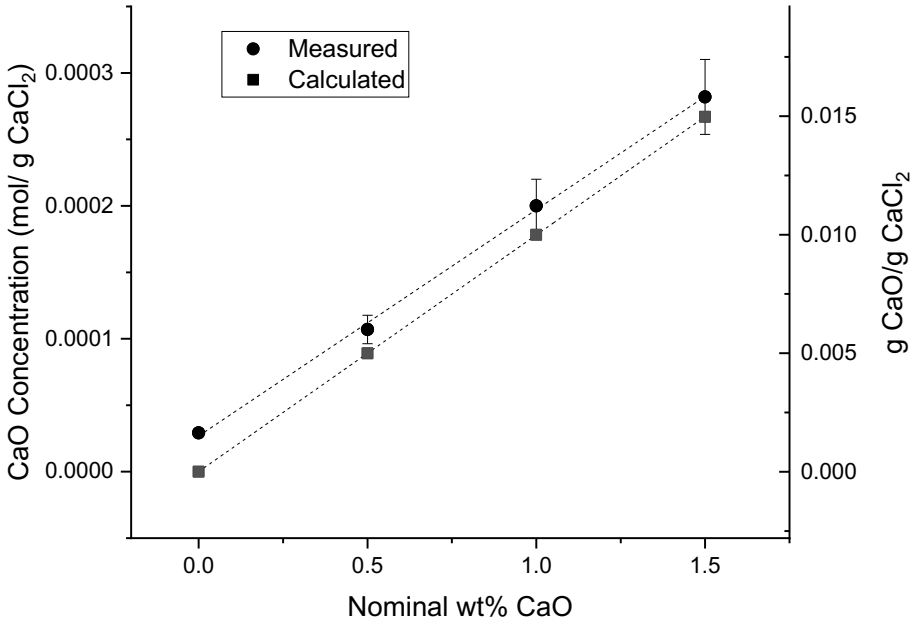

Fig. 4 Titration-measured and calculated CaO concentration in $CaCl_2$ plotted versus the nominal concentration of added CaO in wt%.

From the appearance of the CV plots shown in Figure 3, another method is evident that can be used to measure CaO concentration in molten $CaCl_2$. The oxidation peaks at 0.4 V vs. the quasi-reference electrode increases in magnitude with increasing concentration of added CaO. This is hypothesized to be due to the following family of reactions, assuming that x can be variable:

$$xO_2^- + W = WO_x + 2xe^- \quad (9)$$

Figure 5 shows an overlay of CV plots for as-received $CaCl_2$ before and after known additions of CaO at a scan rate of 300 mV/s. It makes sense that the oxidation reaction occurs at a slightly higher potential than the reference electrode potential, since W is the reference electrode.

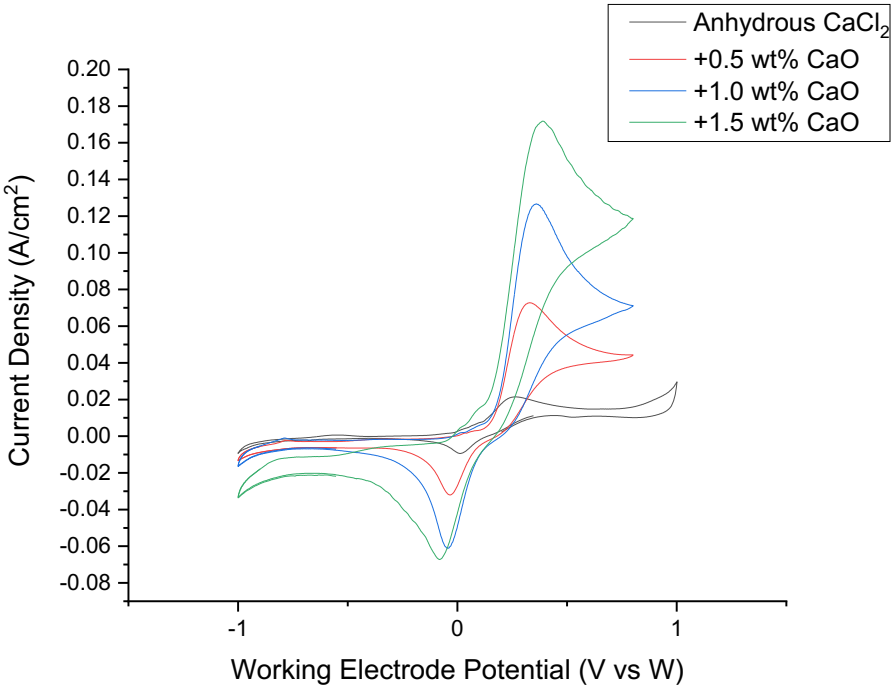

Fig. 5 Cyclic voltammograms of anhydrous $CaCl_2$ with CaO added in 0.5 wt% increments. Scans were performed at a scan rate of 300 mV/s at a temperature of 850°C. Tungsten was used for all three electrodes, and theWE had a diameter of 2 mm.

CVs were also run for each salt mixture at multiple scan rates ranging from 50 to 400 mV/sec. The current density of the oxidation peak was plotted vs. the square root of the scan rate (Figure 6). A fit through the origin would mean that reactions are reversible and the slope of this line vs. concentration could be used to estimate the initial concentration of CaO present in the salt using the Berzins-Delahay equation. As the lines do not appear to fit through the origin, save for pure $CaCl_2$, the Berzins-Delahay equation was not used. Based on repeat measurements, the current measurement error is estimated to be 1%.

Rather than using the Berzins-Delahay equation to correlate oxidation current density with oxide ion concentration, peak current density at a fixed scan rate was plotted against the added concentration of O^{2-} in the salt. This plot is shown in Figure 7. The negative of the y-intercept value was taken as the initial concentration. This method indicated 0.2 wt% concentration of CaO in the as-received anhydrous $CaCl_2$, or 3.57 x 10^{-5} mol CaO/g salt. This compares closely with the

CaO concentration in as-received anhydrous $CaCl_2$ determined by titration (3.0×10^{-5} mol CaO/g salt). Thus, either titration or CV of molten $CaCl_2$ appears to be viable for measurement of the oxide concentration term needed for Equation (5).

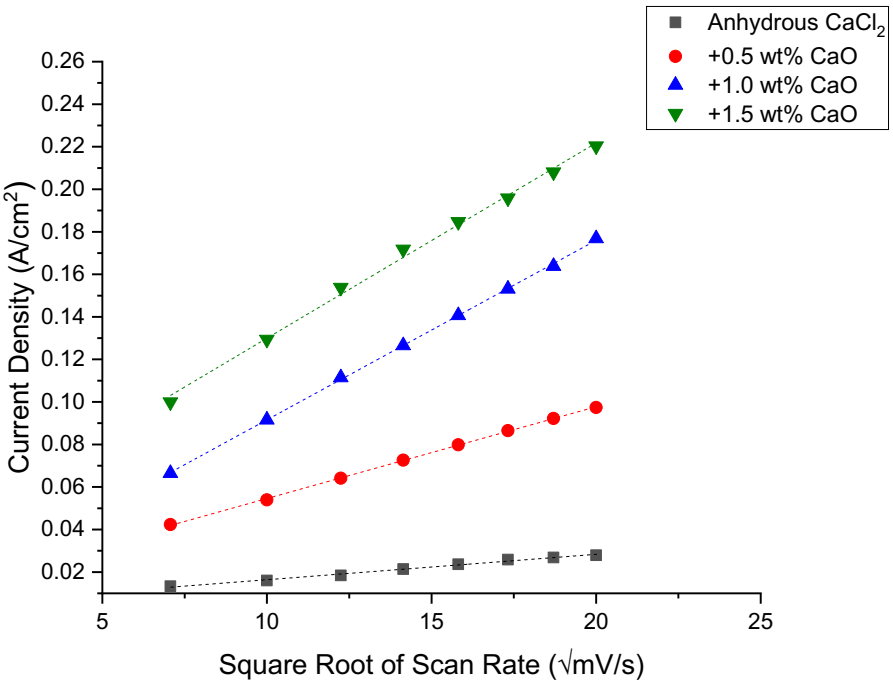

Fig. 6 Plot of the peak magnitude vs. the square root of the scan rate for anhydrous $CaCl_2$ with three levels of addition of CaO. T = 850°C.

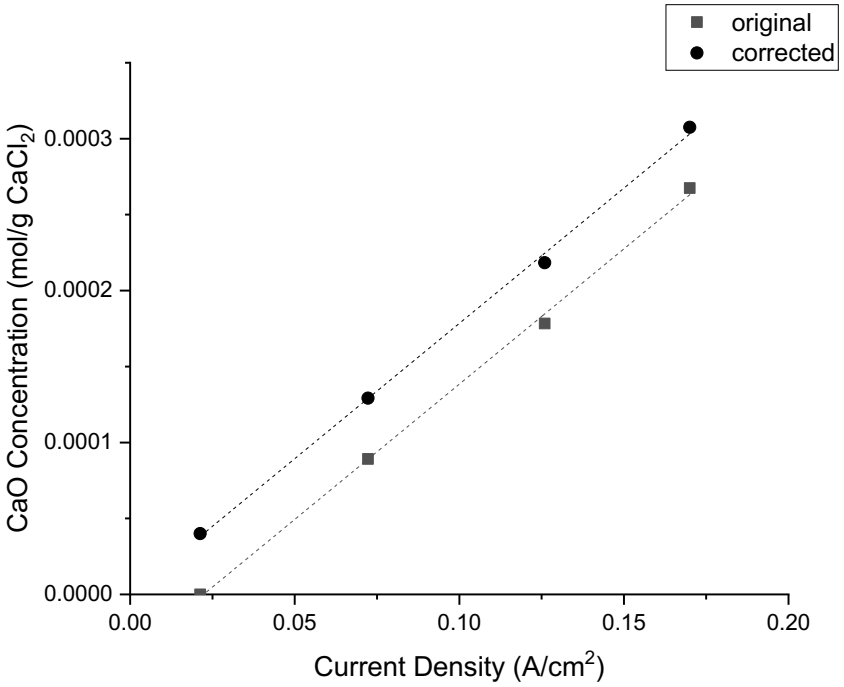

Fig. 7 Plot of the concentration of added CaO to the current density of the CV oxidation peak. Scan rate = 300 mV/s, T = 850°C. Tungsten rods were used for WE, CE, and RE. The WE had a diameter of 2 mm.

It is thus apparent that three methods (thermogravimetric analysis, titration, and cyclic voltammetry) can be combined to quantify water contamination in a sample of $CaCl_2$. TGA of as-received salt yields the concentration of desorbable water (C_{des}). A melted salt sample can then be titrated to give the concentration of CaO (C_{oxide}). The CaO concentration can also be obtained with CV of $CaCl_2$.

This method of calculation can be applied to the results presented previously in this paper. The mass loss from unreacted water, defined as that measured by TGA before 370°C, was 1.41 x 10^{-4} mol CaO/g $CaCl_2$. This value represents C_{des} in Equation (5). This can be combined with either the CV or titration results (representing C_{oxide}) to give a total initial CaO concentration. The CV result, an estimated 3.57 x 10^{-5} mol CaO/g $CaCl_2$ as shown in Figure 7, yields a value of 1.8 x 10^{-4} mol CaO/g $CaCl_2$ for C_{tot}. The second approach is to use the 3.0 x 10^{-5} mol CaO/g $CaCl_2$ from titration, which when combined with the concentration found through TGA, would give an

342 estimated concentration (C_{tot}) of 1.7x10^{-4} mol CaO/g $CaCl_2$ in the anhydrous salt. These two
343 methods are in good agreement with each other.

344

345 *Reaction of O^{2-} with Dissolved Metal Chlorides*

346 The anticipated effect of residual water and ultimately oxide ions on actinide
347 electrorefining in molten $CaCl_2$ is the reaction of the oxide ions with dissolved actinide chlorides.
348 If electrorefining U, Pu, or spent nuclear fuel, UCl_3 or $PuCl_3$ would need to be maintained in the
349 molten $CaCl_2$ to maintain a high rate of electrorefining. To test the interaction that residual water
350 contamination would have with various dissolved actinide chlorides, $CeCl_3$ was added as a
351 surrogate for UCl_3 or $PuCl_3$ to molten $CaCl_2$-CaO mixtures. Cerium was selected as a surrogate
352 based on the similarity of its standard reduction potentials for oxide and chloride states to those
353 for plutonium. Furthermore, both cerium and plutonium are only state in the +3 oxidation state in
354 molten $CaCl_2$. Postulated reactions are as follows:

355

356 $$2CeCl_3 + 3CaO \rightarrow Ce_2O_3 + 3CaCl_2 \quad (10)$$

357 $$CeCl_3 + CaO \rightarrow CeOCl + CaCl_2 \quad (11)$$

358

359 If either of these reactions is spontaneous in the molten $CaCl_2$ at 850°C, additions of $CeCl_3$ would
360 lower the magnitude of the CV oxidation peak using W as the working electrode. Once all of the
361 CaO has been reacted, new peaks should appear due to Ce^{3+} reduction and Ce oxidation. Figure 8
362 shows CVs of $CaCl_2$ initially with 1.5 wt% CaO plus this salt mixture with additions of $CeCl_3$.
363 Two levels of $CeCl_3$ addition were tested (1 and 5 wt%). Both oxidation and reduction peaks
364 previously associated with CaO decrease in magnitude with the addition of $CeCl_3$. Two very small
365 oxidation peaks at about -0.8 V appear in the CVs done after adding $CeCl_3$. This position in the
366 CV is consistent with Ce metal oxidation. Thus, there appears to be some residual $CeCl_3$ in the salt
367 that reduces onto the working electrode when the potential is decreasing and then oxidizes when
368 the potential is increasing. Since the Ce oxidation peaks are so small, it suggests that one or both
369 of the above reactions, represented by Equations (7) and (8), are occurring to some extent. Figure
370 9 further demonstrates the response of the oxidation curve to the addition of $CeCl_3$. $CeCl_3$ was

added in two 1 wt% increments to anhydrous $CaCl_2$. Again, there was a reduction in the peak height. Interestingly, no Ce oxidation peaks were observed in Figure 9. It is important to keep in mind that these CVs were run using a W quasi-reference electrode. The potentials are subject to shifting, therefore, as the redox potential of the salt changes. The reference potential is not fixed. As can be seen in Figures 8 and 9, there appears to be some shifting of the potentials with addition of $CeCl_3$. The green curve in Figure 8 associated with 1.5 wt% CaO and 5 wt% $CeCl_3$ has the Ca^{2+}/Ca reduction peak shifted a small amount to the left compared to the other salt mixtures. Such minor changes in potential do no affect our ability to interpret the CVs.

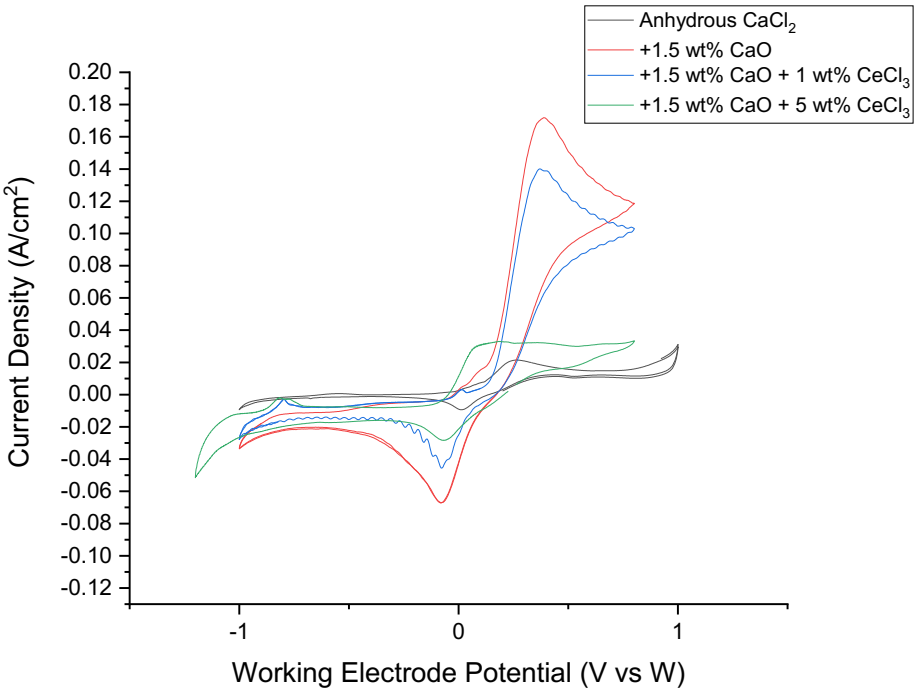

Fig. 8 Cyclic voltammetry of anhydrous $CaCl_2$ with incremental additions of CaO and $CeCl_3$. Scans were performed at 300 mV/s, at 850°C, against a 2 mm diameter tungsten quasi-reference electrode and without correction for uncompensated solution resistance.

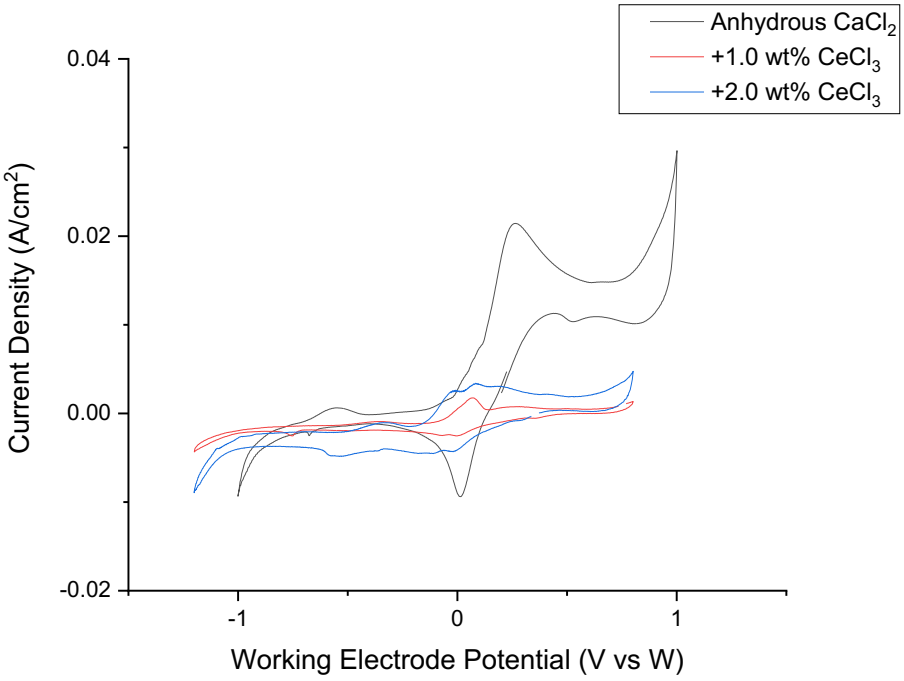

384

385 **Fig. 9** Cyclic voltammetry of anhydrous $CaCl_2$ with incremental additions of $CeCl_3$. Scans were
386 performed at a scan rate of 300 mV/s, at a temperature of 850°C. Tungsten was used for all three
387 electrodes, and the WE had a 2 mm diameter.

388 After CV was run, metallic deposits were observed on the counter and reference electrodes,
389 as shown in Figure 10. The deposits appeared at first to be solidified salt but sparkled and had a
390 rougher texture than typical salt coatings. This coating had not been seen in any previous tests. A
391 likely explanation is that, unlike previous tests with a lower added $CeCl_3$, this melt had $CeCl_3$ still
392 present in the salt. Scanning to a low enough potential caused cerium metal to deposit on the
393 electrodes. There may be underpotential deposition of Ce metal along with Ca metal deposition.

394

Fig. 10 Metallic deposits on the counter and reference electrodes after CV of $CaCl_2$-CaO-$CeCl_3$ salt mixtures.

The $CaCl_2$-CaO-$CeCl_3$ melt was brought to 7 wt% $CeCl_3$ to ensure that more than enough cerium was available to react with all the CaO present. After the salt was cooled and allowed to freeze, the crucible containing 7 wt% $CeCl_3$ was cracked open. A photo of the salt layers is shown in Figure 11. The cross section showed a distinct separation in phases. A sample from the bottom layer (as indicated in Figure 11) was collected for XRD. The most prevalent phase in the mixture was $CaCl_2$ as shown in the XRD, shown in Figure 12, and cerium was present as either Ce_2O_3 or CeOCl. Small amounts of CaO were still present, as was MgO contamination from the crucible. This indicates that as cerium is introduced into CaO-contaminated $CaCl_2$, it forms both insoluble oxide and oxychloride. Such precipitation should also be apparent when using $CaCl_2$ with some residual water initially but without addition of CaO. This was not tested due to estimation that the precipitate layer would not be substantial enough for visual observation and XRD analysis.

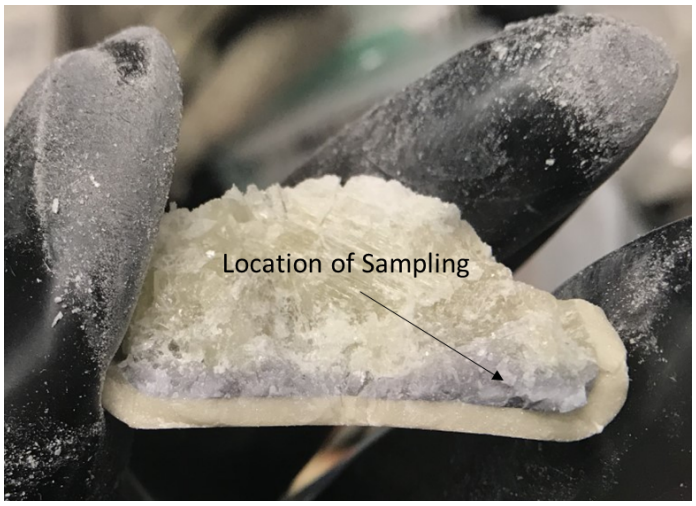

411

412 **Fig. 11** A cross section of the crucible containing $CaCl_2$ and CaO with 5 wt% $CeCl_3$.

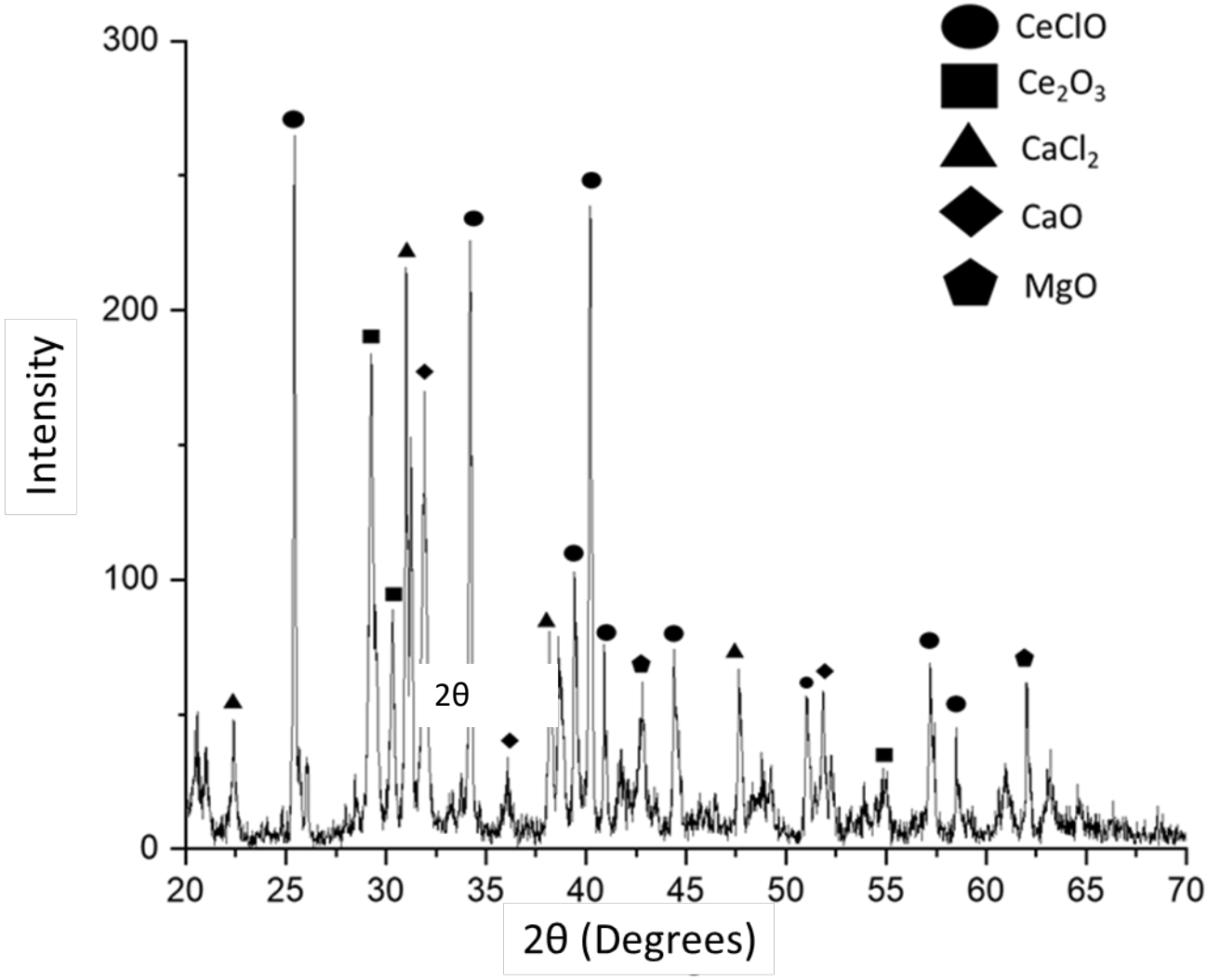

Fig. 12 XRD results showing phases present in the bottom layer of the salt.

ICP-MS was used to measure the cerium concentration for $CaCl_2$ with 1.5 wt% CaO, with an addition of 0.5, 1.0, and 5.0 wt% $CeCl_3$. The results are summarized in Table 1. For both 0.5 and 1.0 wt% $CeCl_3$ additions, the ICP-MS analysis of the salt samples indicated 2.8 x 10^{-5} mol Ce/g salt. As seen in Table 1, these are comparable to the as weighed (nominal) concentrations. That would seem to indicate that CeCl3 is not reacting with CaO. An additional 4 wt% was added to bring the total nominal mixture to 1.5 wt% CaO and 5% $CeCl_3$. This is equivalent to a molar ratio of 0.75 for $CeCl_3$ to CaO. Equation (10) indicates 2 moles of Ce react with 3 moles of CaO, while equation (11) indicates 1 mole of Ce reacts with 1 mole of CaO. Thus, most if not all of the $CeCl_3$

added for each test should have reacted with CaO if reactions (10) or (11) are spontaneous. A sample removed from the furnace 2 hours after bringing up the $CeCl_3$ addition to 5 wt% indicated 1.62×10^{-4} mol $CeCl_3$/g $CaCl_2$, or 81% of what was added. However, after waiting an additional 7 hours, another sample was taken and the concentration was found to be 6.7×10^{-6} mol $CeCl_3$/g $CaCl_2$, or 3.3% of what was added. Thus, given enough time, the $CeCl_3$ will react with CaO to near completion, providing evidence that either insoluble oxide or oxychloride is formed.

Table 1. Nominal versus measured (ICP-MS) concentrations for additions of $CeCl_3$ in $CaCl_2$ with initially 1.5 wt% CaO at 850°C.

Nominal Concentration $CeCl_3$ added (wt%)	Nominal Concentration $CeCl_3$ added (mol Ce/g salt)	Nominal Initial Molar ratio of $CeCl_3$/CaO	Measured Concentration at 2 hr $CeCl_3$ (mol Ce/g salt)	Measured Concentration $CeCl_3$ at 9 hr (mol Ce/g salt)
0.5	2.0×10^{-5}	0.075	2.8×10^{-5}	Not measured
1.0	4.1×10^{-5}	0.15	2.8×10^{-5}	Not measured
5.0	2.0×10^{-4}	0.75	1.62×10^{-4}	6.7×10^{-6}

Conclusions

Removing water from calcium chloride requires conditions to minimize formation of oxides in the salt due to $CaCl_2$ hydrolysis. In this paper, we showed that $Ca(OH)_2$ is not stable in $CaCl_2$ at high temperatures (>400°C) and that CaO is the primary contaminant generated by this hydrolysis reaction. TGA can be used to measure the amount of H_2O that is physically removable from the salt to a given temperature rather than reacting with $CaCl_2$. Both CV and titration can be used to measure CaO concentration after dehydration, thereby accounting for water that has reacted with $CaCl_2$. When the result from TGA is combined with the result from either CV or titration, the total amount of water in as-received $CaCl_2$ salt can be accounted for. Removing CaO from the salt is essential for nuclear material electrochemical processing applications in which metal chlorides are required for optimal processing performance. In this study, through XRD and

444 ICP-MS analysis of reacted $CeCl_3$ and CaO in $CeCl_3$ salt, it was shown that $CeCl_3$ added to salt
445 containing CaO will precipitate to form CeOCl and Ce_2O_3.

446

447 **Acknowlegements**

448 Funding for this project was provided by Los Alamos National Laboratory under subcontract
449 #476229.

450 **References**

451 [1] Rammelberg H, Schmidt T, and Ruck W (2012) Hydration and dehydration of salt
452 hydrates and hydroxides for thermal energy storage—Kinetics and energy release. Energy
453 Procedia. 30: 362–369
454 [2] Ouchi T, Kim H, Spatocco B, and Sadoway D (2016) Calcium-based multi-element
455 chemistry for grid-scale electrochemical energy storage. Nat. Commun. 7: 1–5
456 [3] Sakamura Y, Kurata M, and Inoue T (2006) Electrochemical Reduction of UO_2 in Molten
457 $CaCl_2$ or LiCl. J. Electrochem. Soc. 153: D31–D39
458 [4] Wick O (1967) Plutonium Handbook; a Guide to the Technology. Vol 2. New York:
459 Gordon and Breach.
460 [5] Wade W and Wolfe T (1968) The Production of Plutonium Metal by Direct Reduction of
461 the Oxide. UCRL-50403, Lawrence Radiation Laboratory, University of California,
462 Livermore, California.
463 [6] Iizuka M, Inoue T, Ougier M, and Glatz J (2007) Electrochemical reduction of (U, Pu)O_2
464 in molten LiCl and $CaCl_2$ electrolytes. J. Nucl. Sci. Technol. 44: 801–813
465 [7] Niedrach L and Glamm A (1956) Uranium Purification by Electrorefining. J.
466 Electrochem. Soc. 103: 521
467 [8] Burris L, Steunenberg R, and Miller W (1987) Application of Electrorefining for
468 Recovery and Purification of Fuel Discharged From the Integral Fast Reactor. AIChE
469 Symposium Series. 83: 135–142
470 [9] Smirnov M, Korzun I, and Oleynikova V (1988) Hydrolysis of molten alkali chlorides,
471 bromides and iodides. Electrochim. Acta. 33: 781–788
472 [10] Laitinen H, Ferguson W, and Osteryoung R (1957) Preparation of Pure Fused Lithium

473 Chloride-Potassium Chloride Eutectic Solvent. J. Electrochem. Soc. 104: 516
474 [11] Yan J and Zhao C (2015**)** Thermodynamic and kinetic study of the dehydration process of
475 CaO/Ca(OH)2 thermochemical heat storage system with Li doping. Chem. Eng. Sci. 138:
476 86–92
477 [12] Kariya J (2017) Development of thermal energy storage material using porous silicon
478 carbide and calcium hydroxide. Energy Procedia. 131: 395–406
479 [13] Kondo H, Asaki Z, and Kondo Y (1978) Hydrolysis of Fused Calcium Chloride at High
480 Temperature. Metallurgical Transactions B. 9B: 477-483.
481 [14] Outotec Technologies, HSC Chemistry v.9.
482 [15] Rappleye D, Horvath D, Wang Z, Zhang C, and Simpson M (2016) Methods for
483 Determining the Working Electrode Interfacial Area for Electroanalytical Measurements
484 of Metal Ions in Molten LiCl-KCl. ECS Transactions. 75: 55-61
485